ELSEVIER

Journal of Nuclear Materials 318 (2003) 192–199

journal of nuclear materials

www.elsevier.com/locate/jnucmat

Mechanical properties of modified 9Cr–1Mo (T91) irradiated at $\leqslant 300$ °C in SINQ Target-3

Y. Dai [a,*], X.J. Jia [a], K. Farrell [b]

[a] *Spallation Neutron Source Division, Paul Scherrer Institut, 5232 Villigen PSI, Switzerland*
[b] *Metals and Ceramics Division, Oak Ridge National Laboratory, Oak Ridge, TN 37831, USA*

Abstract

Specimens of martensitic steel T91 were irradiated in the Swiss spallation neutron source (SINQ) Target-3 in a temperature range of 90–300 °C to displacement doses between 3 and 9.8 dpa. Tensile tests were performed at 22, 250 and 350 °C, and small punch (SP) tests were conducted in a temperature range of −186 to 22 °C to derive the change of the ductile–brittle transition temperature ($\Delta DBTT_{SP}$) of the steel after irradiation. The tensile test results demonstrate that the irradiation hardening increases with dose. The uniform elongation falls to less than 1%, while the total elongation is greater than 5% in all cases. All the tensile samples broke in a ductile fracture mode. In the present dose range the irradiation hardening does not saturate and increases even more rapidly at doses above about 6 dpa. The SP tests indicate that the $DBTT_{SP}$ of 0.25 mm thick T91 discs is about −153 °C for the unirradiated condition. After irradiation the $DBTT_{SP}$ increases significantly to −35 °C at 9.4 dpa, corresponding to an estimated $DBTT_{CVN}$ shift of 295 °C; and meanwhile the upper energies decrease. The $\Delta DBTT_{SP}$ has a linear dependence on helium content. Analyses of the data indicate that the radiation hardening and the occurrence of intergranular fracture mode in the higher dose SP tests are dependent on gas content.

1. Introduction

High-chromium martensitic steels have high strength at elevated temperatures, low thermal stress and anticipated low liquid metal corrosion rates; they are under consideration as tentative materials for the liquid metal containers of high power spallation targets [1,2].

Among the different types of martensitic steels, the 7–9Cr martensitic grades are considered better than those martensitic steels with higher (10–13 wt%) chromium contents because of their lower ductile–brittle transition temperature (DBTT) shifts after irradiation [3,4]. Furthermore, they have a large existing database developed from studies for applications in nuclear power plants and fusion reactors. The modified 9Cr–1Mo martensitic steel, T91 has been selected as the first candidate material for the liquid metal container of the future accelerator driven systems demonstrator and is being widely studied in the European 5th Framework Program. For the same reasons, T91 has been selected as the material for the liquid metal container of the target for the megawatt pilot experiment (MEGAPIE) [5], which will be irradiated at the Swiss Spallation Neutron Source (SINQ) in 2005. Although a significant database exists for T91 after neutron irradiation, the behaviour of the steel under spallation type irradiation is still not well understood. Therefore the investigation of T91 under proton and neutron mixed spectrum irradiation is one of the most important scientific support studies for developing the MEGAPIE target. The present paper will present the preliminary results of tensile and small-punch (SP) tests on T91 irradiated in SINQ Target-3 (also called STIP-I, i.e. the first SINQ target irradiation program) at temperatures $\leqslant 300$ °C to 9.8 dpa.

* Corresponding author. Tel.: +41-56 310 4171; fax: +41-56 310 2485.
E-mail address: yong.dai@psi.ch (Y. Dai).

0022-3115/03/$ - see front matter © 2003 Elsevier Science B.V. All rights reserved.
doi:10.1016/S0022-3115(03)00100-4

2. Experimental

The T91 samples were supplied by Oak Ridge National Laboratory. The material is from Heat 30176. The samples were manufactured from a 3-mm-thick plate, previously cold-rolled from a 6-mm-thick plate. The final heat treatment was: normalized at 1040 °C for 1 h, rapidly cooled, and then tempered at 760 °C for 1 h. The composition of the material is: 8.32 Cr, 0.09 Ni, 0.86 Mo, 0.48 Mn, 0.20 V, 0.06 Nb, 0.092 C, 0.15 Si, 0.012 P and 0.055 N in wt%, balance Fe.

The tensile samples are a miniature type originally proposed for the application in the fusion materials community [6]. The dimensions of the specimen are shown in Fig. 1. The samples were cut along the rolling direction of the plates with an EDM machine, then polished mechanically to the final thickness of 0.4 mm. SP discs are 3 mm diameter and 0.25 mm thick. These discs were prepared in the same way as the tensile samples. There were no additional heat treatments for all the samples before irradiation.

The irradiation was performed in SINQ Target-3 with an incident beam of 570 MeV protons during 1998 and 1999. Detailed information for the irradiation can be found in [7]. The samples were placed in rod 1 and rod 10 in the target. The samples in rod 1 were irradiated in a temperature range of 90–360 °C to a maximum dose of 12.1 dpa. However, a lot of samples in the peak flux region were lost during an unintentional, short overfocus beam excursion. The T91 samples were irradiated outside of this region and received a maximum dose of 9.8 dpa at temperatures up to 290 °C. The irradiation was performed with a total proton current of about 0.85 mA for the first 12 months and about 1.04 mA for the last 2 months of actual beam time. The difference in irradiation temperature in these two periods is as large as 20% of the temperature values. The temperature values reported here are the average values of those in the two periods. Irradiation details for all the samples used in the present study are given in Table 1, which includes the calculated displacement (dpa), helium (He) and hydrogen (H) concentrations, and irradiation temperatures. More details of the dpa, He and H calculation are presented in [8].

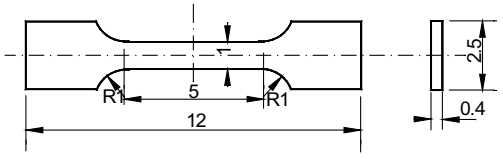

Fig. 1. Dimensions (in mm) of the tensile specimen.

Most of the tensile samples were tested at 250 °C. For comparison, some samples were tested at room temperature. Only one sample was tested at 350 °C, which is higher than the irradiation temperature. The tensile tests were performed on a 2 kN MTS machine at a strain rate of about 1×10^{-3} s^{-1} in flowing Ar gas.

SP tests were performed in a temperature range from ~−186 °C to 22 °C. Fig. 2 illustrates schematically the experimental set-up which is installed in a 10kN Twick tensile test machine. The 3-mm-diameter disc sits atop a 1.5 mm hole in the anvil and is held around its edges with a cylindrical clamp containing a 1.0 mm passage The disc is deformed by pressing a hard steel ball of 1.0 mm diameter into it through the 1.0 mm hole. During deformation the displacement at the centre of the disc can be measured with the extensometer inserted from the hole below the disc. However, for most of the tests the displacement is measured using the cross-head travel value which is calibrated with the extensometer measurement. For a test at a low temperature, the disc and the set-up are cooled with liquid nitrogen directly. The test is started after about 10 min when the temperature is relatively stable. During testing the temperature increases about 2 °C since no additional liquid nitrogen is added after starting the test. A detailed description of the SP tests is given elsewhere [9].

Table 1
Irradiation conditions and tensile test results of T91 tensile specimens

ID	T_{irr} (°C)	dpa	He (appm)	T_{test} (°C)	YS (MPa)	UTS (MPa)	UE (%)	TU (%)	ΔYS (MPa)
I35		0	0	20	551	687	6.25	14.5	
I17		0	0	20	546	680	5.84	14.3	
I20	91	3	180	20	908	910	0.75	8.3	359
I13	194	5.9	390	20	949	955	0.72	8.1	400
I22		0	0	250	484	587	4.57	11.87	
I40	95	3	180	250	702	710	0.98	7.33	218
I23	194	5.9	390	250	754	768	1.17	7.07	270
I12	216	7.6	565	250	843	858	1.29	8.35	359
I06	300	9.8	815	250	900	904	0.89	5.72	416
I32		0	0	350	464	563	3.27	10.6	
I50		0	0	350	475	565	3.34	10.0	
I05	285	9.8	815	350	871	874	0.76	5.7	401

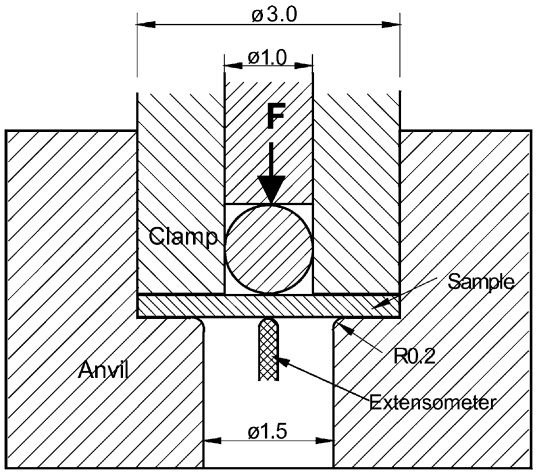

Fig. 2. Sketch showing the central part of the set-up for SP testing.

3. Results

3.1. Tensile tests

Examples of the tensile stress–strain curves are shown in Fig. 3, including those from unirradiated samples. The results of unirradiated samples tested at 22 and 350 °C show a good repeatability of tests. Although only a few samples were tested, the results at 22 and 250 °C demonstrate that the irradiation hardening increases with increasing dose. As is normally observed for irradiated martensitic samples tested at low temperatures (e.g. [10–15]), the samples started to neck immediately after yielding. This leads to a short uniform elongation of less than 1%, although the total elongation is greater than 5% in all cases. Compared to the two irradiated samples tested at 22 °C, the two samples tested at 250 °C with the same doses of 3.0 and 5.9 dpa are considerably weaker and slightly less ductile. Fig. 4 shows pictures of an unirradiated sample and the 9.8 dpa sample, both

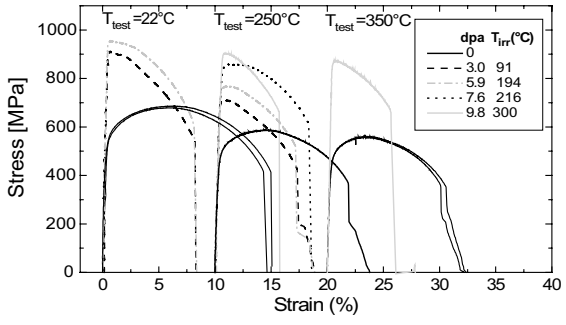

Fig. 3. Engineering tensile stress–strain curves of T91 irradiated at SINQ Target-3 and tested at 22, 250 and 350 °C.

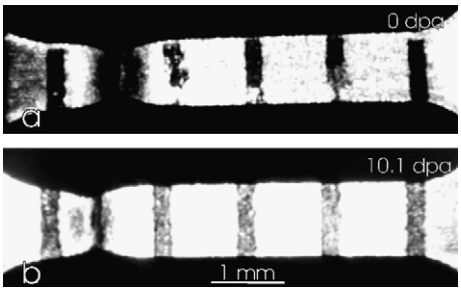

Fig. 4. Pictures of samples tested at 250 °C (a) unirradiated and (b) irradiated to 9.8 dpa. The black lines on the surfaces of the specimens were used for measuring elongation with a video-extensometer.

tested at 250 °C. Necking is quite evident in both specimens. Hence, it is believed that all the tensile samples broke in a predominantly ductile fracture mode.

3.2. Small punch tests

For each irradiation dose, up to 6 SP specimens were tested. Fig. 5(a) shows the load–displacement curves of unirradiated specimens tested in a temperature range from −186 to 22 °C. It can be seen from change of the load–displacement curves that discs are ductile at $\geqslant -150$ °C but become brittle when the temperature is −168 °C and below. This indicates that the $DBTT_{SP}$ of the unirradiated discs is below −150 °C. For irradiated specimens, a similar set of curves was obtained at each dose. As an example, Fig. 5(b) displays the curves of the specimens irradiated to 9.4 dpa and containing about 770 appm He. In this case, the disc shows brittle fracture at −40 °C and below. This indicates that the DBTT has been increased significantly by the irradiation.

Fig. 6 illustrates the temperature dependence of the energy to break the discs. It demonstrates clearly that the temperature–energy curve shifts to higher temperatures as a result of irradiation. The $DBTT_{SP}$ is taken to be the point at which the energy reaches half of the maximum upper shelf energy (USE_{SP}). Fig. 7 shows the dose dependencies of the $DBTT_{SP}$ and EUS_{SP} which indicate that the $DBTT_{SP}$ of T91 steel increases strongly from about −153 °C for the unirradiated condition to about −35 °C after irradiation to 9.4 dpa, whereas the USE_{SP} decreases gradually with increasing dose (Table 2).

After the punch tests, some of the specimens were examined with a scanning electron microscope (SEM) to identify the fracture mode. Fig. 8 presents the SEM micrographs of unirradiated specimens tested at 22, −70, −130 and −186 °C. It can be seen that the fracture mode changes gradually from shallow ductile tearing at 22 °C to a mixed mode of intergranular separation and tough cleavage at −186 °C. For irradiated specimens, with increasing DBTT, this change takes place in a much higher

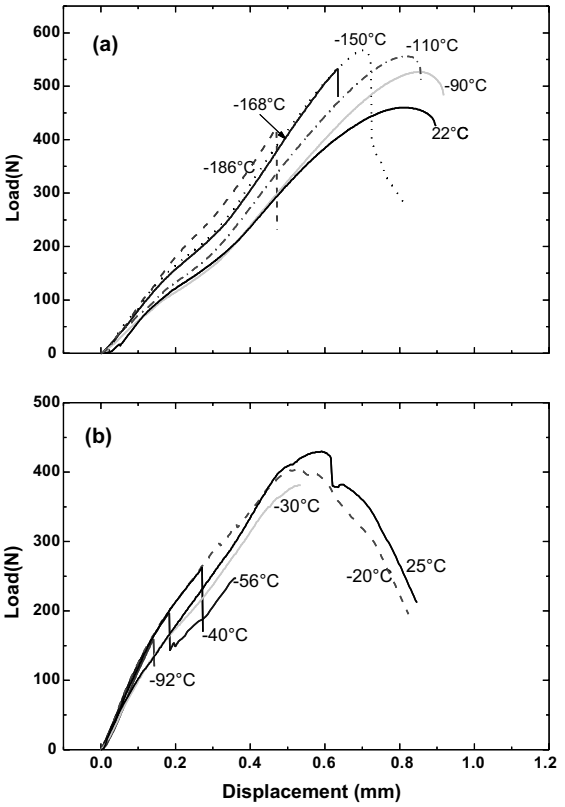

Fig. 5. The load–displacement curves for SP tests of (a) unirradiated specimens and (b) specimens irradiated to 9.4 dpa. Test temperatures are shown on the curves.

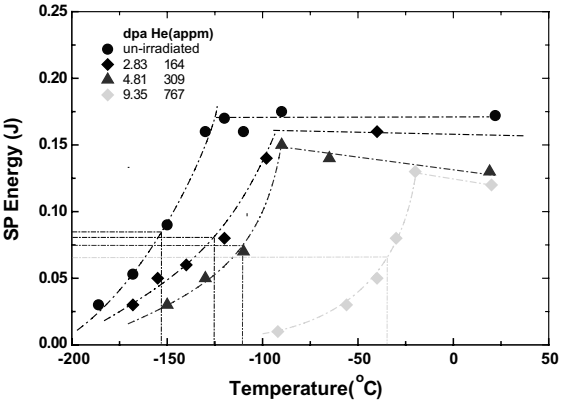

Fig. 6. Test temperature dependence of the SP energy for specimens of different irradiation doses.

temperature range. Fig. 9 demonstrates that the fracture of 9.4 dpa specimens changes quickly from a dominantly transgranular ductile fracture mode at 20 °C to a completely interfacial fracture mode at −30 °C. In the later case, large cracks were observed on the bottom (tension)

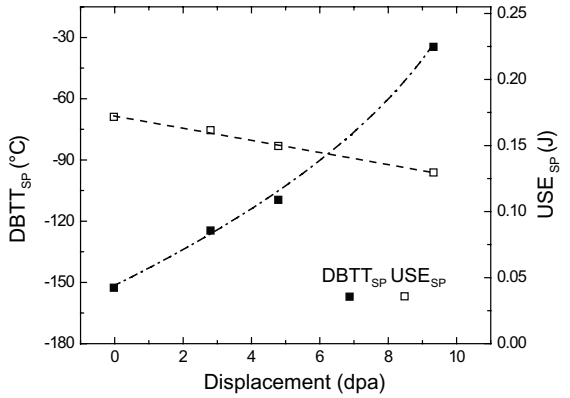

Fig. 7. Irradiation dose dependence of the $DBTT_{SP}$ and USE_{SP}.

surface of the specimen, which propagated along prior austenitic grain boundaries and martensite lath boundaries.

4. Discussion

Martensitic steels irradiated in spallation spectra have been studied intensively recently. At PSI the tensile properties and microstructure of martensitic steels DIN1.4926, F82H, Optimax (a type of 9Cr–1WTa reduced-activation steel) have been investigated. All three steels were irradiated in the 800 MeV proton beam at the Los Alamos Neutron Scattering Center (LANSCE). The steel DIN1.4926 was irradiated in a form of a beam window to a maximum dose of 6.9 dpa at temperatures below 230 °C [11], while the samples of F82H and Optimax steels were irradiated up to 7.8 dpa at 60 °C and below [12]. At Oak Ridge and Los Alamos National Laboratories, T91 and 9Cr–2WTa steels have been studied [14,15]. The samples were irradiated at LANSCE but to a maximum dose of 10.1 dpa. The irradiation was at 160 °C and below. The tensile specimens of the present study were irradiated in a wider temperature range up to 300 °C to a similar maximum dose of 9.8 dpa. TEM observations high-density helium bubbles formed in samples irradiated to about 10 dpa at temperatures above 200 °C [16,17]. In the samples irradiated at LANSCE to lower doses at lower temperatures, no bubbles were observed [12]. Therefore, it is interesting to compare the present results with those from LANSCE irradiation. For simplicity the comparison is limited to results of T91 steel only.

In Fig. 10, the yield stress (YS), ultimate tensile strength, uniform elongation and total elongation of T91 irradiated in LANSCE and SINQ targets and tested at different temperatures are plotted as a function of irradiation dose. For the control test at room temperature, both YS and tensile strength data from the present work agree well with other data [14] for the same heat of

Table 2
Irradiation conditions and SP test results of T91 SP specimens

ID	T_{irr} (°C)	dpa	He (appm)	$DBTT_{SP}$ (°C)	$\Delta DBTT_{SP}$ (°C)	USE (J)
		0	0	−153		0.171
Ia	90	2.8	165	−125	28	0.161
Ib	159	4.8	310	−110	43	0.149
Ie	275	9.4	765	−35	118	0.129

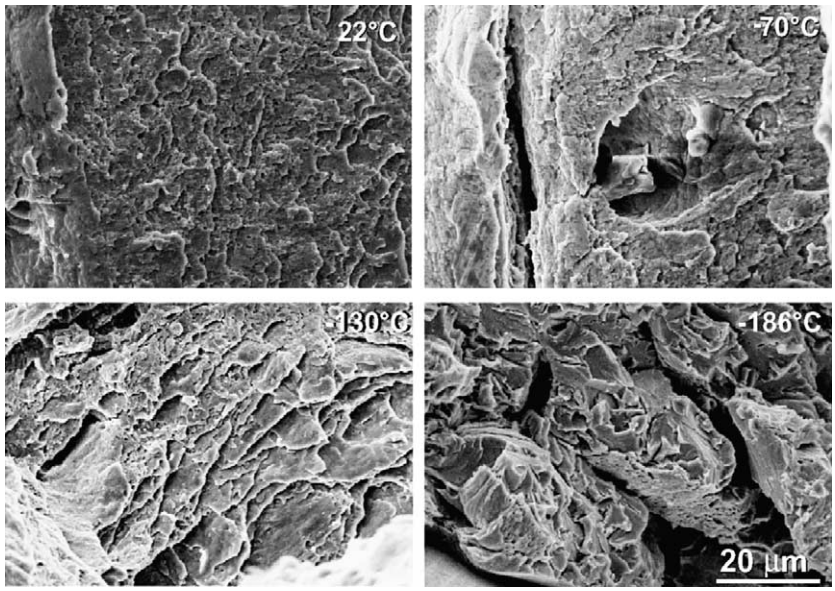

Fig. 8. SEM micrographs showing the fracture surfaces of unirradiated SP specimens tested at 22, −70, −130 and −186 °C.

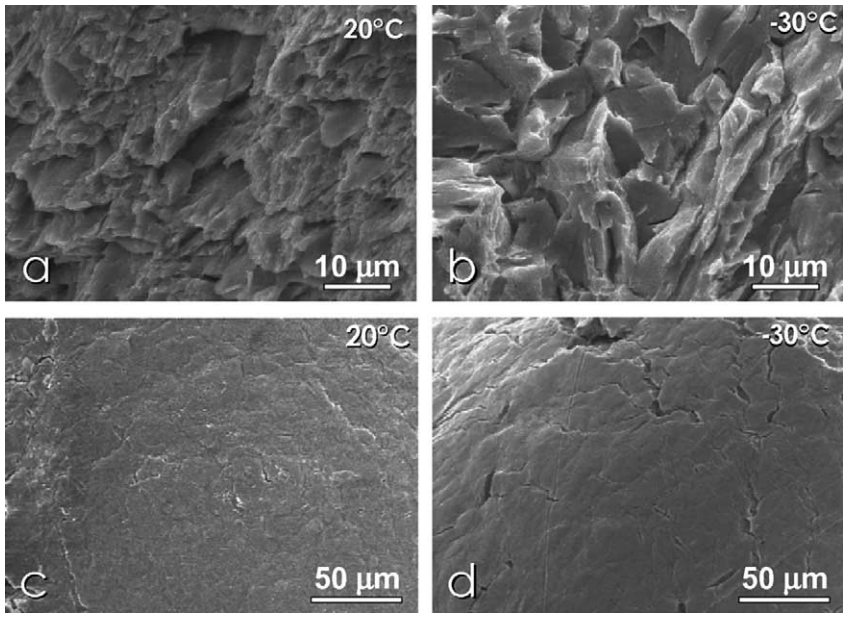

Fig. 9. SEM micrographs showing (a) and (b) the fracture surfaces, (c) and (d) the lower surfaces (see Fig. 1) of SP specimens irradiated to 9.4 dpa and tested at 20 and −30 °C.

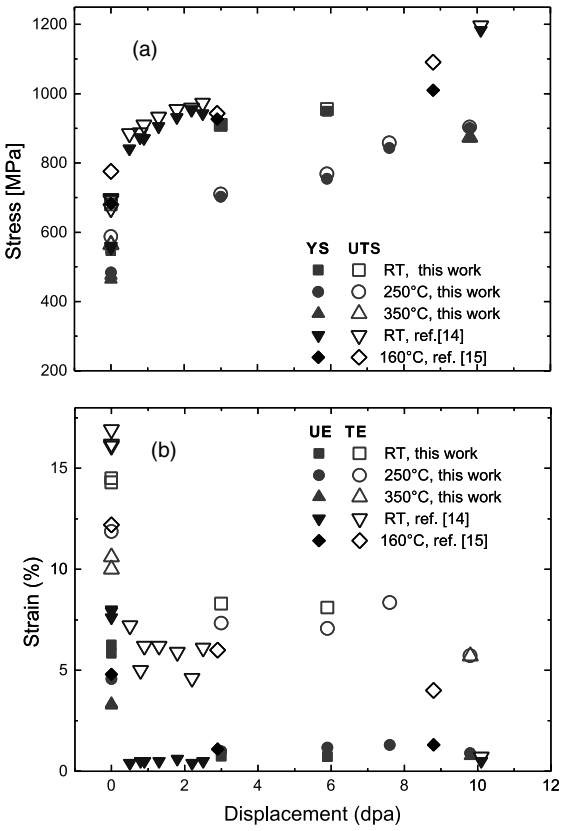

Fig. 10. Irradiation dose dependence of (a) YS and ultimate tensile strength, and (b) uniform elongation and total elongation of T91 irradiated in LANSCE and SINQ targets and tested at different temperatures.

steel. The slight differences between the elongation values (Fig. 10(b)) can be attributed to differences in specimen geometry. Fig. 10(b) demonstrates that the uniform elongations of all the irradiated samples, regardless of their irradiation temperatures and doses and testing temperatures, are low, 0.5–1%. The total elongation does not change much between about 0.5 and about 8 dpa, after which it falls abruptly to about 1%. This trend will be investigated with samples of higher dose from the second SINQ target irradiation program (STIP-II) in the future. The total elongation of SINQ irradiated samples is overall slightly greater that of LANSCE irradiated ones. This may be attributed to the different irradiation environments.

TEM investigation of these specimens shows that helium bubbles of about 1.2 nm diameter with a density of 5.4×10^{23} m^{-3} formed in a TEM disc irradiated to 9.8 dpa [17]. It is pertinent to discuss whether such small helium bubbles introduce significant hardening.

The general observations on bcc and fcc metals irradiated with neutrons, protons or ions to low dose levels in the low-temperature regime $T_i \leqslant 0.3T_m$ (T_m is the absolute melting point) show that radiation hardening, indicated by an increase in YS ($\Delta\sigma_y$), is related to the irradiation dose (dpa) by an expression of the form $\Delta\sigma_y \propto (\text{dpa})^n$, where $1/4 \leqslant n \leqslant 1/2$ [11,12,18–20]. This relationship is usually explained in terms of a dispersed barrier hardening mechanism in which $\Delta\sigma_y \propto \alpha b\mu(Nd)^{1/2}$, where α is the strength of the barrier, b is the Burgers vector of mobile dislocations, μ is the shear modulus of the material, and N and d are the number density and size of the barriers [21,22]. The barriers can be radiation-induced dislocation loops, stacking fault tetrahedra, precipitates, voids, or gas bubbles, each with different α values. If the (Nd) product scales linearly with dose, the dose exponent, n, in the $\Delta\sigma_y \propto (\text{dpa})^n$ relationship will be 1/2, as is found for irradiated copper single crystals [22]. If (Nd) varies as $(\text{dpa})^{1/2}$, as is found for irradiated copper polycrystals [23], n will be 1/4. Such exponents will be meaningful only at doses below the doses where the barriers remain discrete and continue to be developed with increasing dose. Saturation will occur when the barriers begin to be eroded by overlap of displacement cascades. Then the exponent should decline. Fig. 11 shows a comparison between neutron- and proton-irradiated T91. For T91 irradiated with neutrons at 50 °C, the $\Delta\sigma_y$ saturates at about 7 dpa [10], while for proton-irradiated T91 at a similar temperature, the $\Delta\sigma_y$ does not saturate at doses up to 10 dpa, and meanwhile the value is also significantly greater than that of neutron irradiation. Furthermore, the present data from the tests at 250 °C show that the increase in YS has a slope of about 1/4 at doses of 3–6 dpa above which, instead of a decline, the slope approaches unity. This evidence implies that additional barriers are forming. The most likely source of continuously developing barriers at these high doses around the cascade overlap dose is the high concentration of gas bubbles associated with the high gas production rates in spallation irradiations.

The hardening produced by irradiation-induced dislocation loops alone can be modeled by $\Delta\sigma_y \propto$

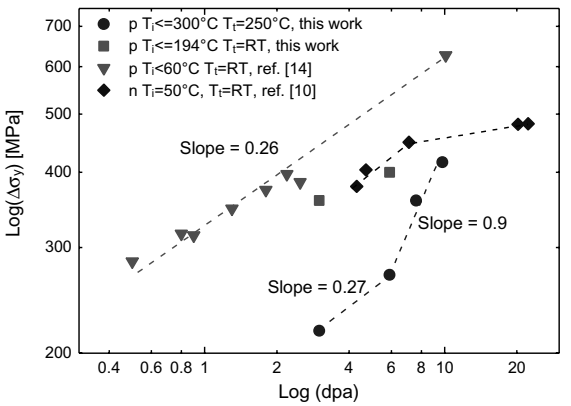

Fig. 11. Irradiation dose dependence of the increase of YS after irradiation.

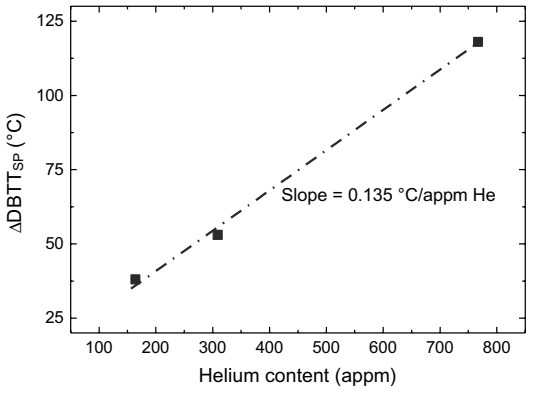

Fig. 12. Helium content dependence of the $\Delta DBTT_{SP}$ of T91.

$\alpha b\mu(Nd)^{1/2}$. From the data of T91 at a similar dose presented in [17], the densities and sizes of dislocation loops at 3.2, 6.2 and 9.8 dpa are 2.1×10^{22} m^{-3}/2.6 nm, 1.9×10^{22} m^{-3}/4.5 nm, 3.3×10^{22} m^{-3}/5.4 nm, respectively. These numbers provide ratios of $(Nd)^{1/2}$:1:1.25:1.81. The corresponding ratios of $\Delta\sigma_y$ are 1:1.24:1.91. These indicate that the hardening at 9.8 dpa dose cannot be assigned solely to the hardening induced by dislocation loops. In fact, at 9.8 dpa, the value of $(Nd)^{1/2}$ for bubbles is about double for loops. This means bubbles can contribute significant hardening even if they are very weak barriers [24].

The results of the small punch (SP) testing of the present study are very interesting in the sense that they indicate an effect of helium on the DBTT shift. The correlation between the DBTT shift of SP tests ($\Delta DBTT_{SP}$) and that of Charpy impact tests ($\Delta DBTT_{CVN}$) can be roughly expressed as $\Delta DBTT_{CVN} \cong 2.5\Delta DBTT_{SP}$ [9]. Calculating from the $\Delta DBTT_{SP}$ values we obtain 95, 133 and 295 °C for $\Delta DBTT_{CVN}$ at 2.8, 4.8 and 9.4 dpa, respectively. Such a large increase of DBTT has not been observed in fast neutron irradiated T91, where $\Delta DBTT_{CVN}$ saturates at about 50 °C after irradiation at 390 °C [25]. However, when helium is present in martensitic steels, the DBTT can be significantly increased. An increase of more than 200 °C was observed in T91 Charpy samples irradiated in a mixed neutron spectrum at HFIR [26], where 30 appm helium was produced. The large increase was associated with the onset of intergranular fracture. Helium effects on DBTT shift have been also observed in a number of martensitic steels irradiated in HFR, where the DBTT increases with the helium content (transformed from boron) in the steels after irradiated to 0.8 dpa [27]. In the present study, the $\Delta DBTT_{SP}$ shows a linear increase with helium content, as illustrated in Fig. 12. Such phenomena have also been observed in martensitic steels F82H and Optimax-A [9]. This correlation, coupled with our observation of extensive cracking on prior austenite and lathe boundaries, implies that the high DBTT values may be greatly promoted by the presence of the spallation-produced gases.

5. Conclusion

Specimens of martensitic T91 steel were irradiated at SINQ Target-3 in a temperature range of 90–300 °C up to 9.8 dpa. Tensile tests were performed at 22, 250 and 350 °C, and SP tests were conducted in a temperature range of −186 to 22 °C. The tensile test results show that:

(a) The irradiation hardening increases with increasing dose. The uniform elongation drops to less than 1%, while the total elongation is greater than 5% in all cases. All the samples broke in a ductile fracture mode.
(b) At doses below about 6 dpa, $\Delta\sigma_y$ is proportional to $(dpa)^{0.27}$, while at higher doses it is proportional to $(dpa)^{0.9}$. It is suggested that a high density of gas bubbles contributes to radiation hardening above 6 dpa.

The results of the SP tests indicate that:

(a) The $DBTT_{SP}$ of T91 SP samples is about −153 °C for the unirradiated condition. After irradiation, the $DBTT_{SP}$ increases while the USE_{SP} decreases significantly. The shift in $DBTT_{SP}$ at 9.4 dpa is equivalent to a Charpy DBTT shift of 295 °C.
(b) The $\Delta DBTT_{SP}$ has a linear dependence on the helium contents of the samples, and there is intergranular cracking at 9.4 dpa and 765 appm He. These factors are taken to indicate strong effects of helium on the ductile brittle transition of this martensitic steel.

Acknowledgements

The authors would like to express thanks to Mr R. Thermer for his help on experiments. This work is included in both SPIRE (Irradiation effects in martensitic steels under neutron and proton mixed spectrum) subprogram of the European 5th Framework Program and ESS TMR program, which are supported by Swiss Bundesamt für Bildung und Wissenschaft.

References

[1] Y. Dai, in: Proceedings of ICANS-XIII and ESS-PM4, 11–19 October 1995, PSI, p. 604.

[2] R.L. Klueh, in: Proceedings of 1st International Workshop on Spallation Materials Technology, 23–25 April 1996, Oak Ridge, p. 3.3–19.
[3] R.L. Klueh, D.J. Alexander, in: Effects of Radiation on Materials: 16th International Symposium, ASTM STP 1125, 1992, p. 1256.
[4] A. Kohyama, A. Hishinuma, D.S. Gelles, R.L. Klueh, W. Dietz, K. Ehrlich, J. Nucl. Mater. 233–237 (1996) 138.
[5] J.L. Boutard, Y. Dai, K. Ehrlich, MEGAPIE general meeting.
[6] P. Jung, A. Hishinuma, G.E. Lucas, H. Ullmaier, J. Nucl. Mater. 232 (1996) 186.
[7] Y. Dai, G.S. Bauer, J. Nucl. Mater. 296 (2001) 43.
[8] Y. Dai, Y. Foucher, M. James, B. Oliver, these Proceedings. doi:10.1016/S0022-3115(03)00099-0.
[9] X. Jia, Y. Dai, in press.
[10] R. Klueh, J.M. Vitek, J. Nucl. Mater. 161 (1989) 13.
[11] Y. Dai, F. Carsughi, W.F. Sommer, G.S. Bauer, H. Ullmaier, J. Nucl. Mater. 276 (2000) 289.
[12] Y. Dai, S.A. Maloy, G.S. Bauer, W.F. Sommer, J. Nucl. Mater. 283–287 (2000) 513.
[13] A.F. Rowcliffe, J.P. Robertson, R.L. Klueh, K. Shiba, D.J. Alexander, M.L. Grossbeck, S. Jitsukawa, J. Nucl. Mater. 258–263 (1998) 1275.
[14] K. Farrell, T.S. Byun, J. Nucl. Mater. 296 (2001) 129–138.
[15] S.A. Maloy, M.R. James, G. Willcutt, W.F. Sommer, M. Sokolov, L.L. Snead, M.L. Hamilton, F. Garner, J. Nucl. Mater. 296 (2001) 119.
[16] X. Jia, Y. Dai, M. Victoria, J. Nucl. Mater. 305 (2002) 1.
[17] X. Jia, Y. Dai, these Proceedings. doi:10.1016/S0022-3115(03)00101-6.
[18] N. Baluc, C. Bailat, Y. Dai, M.I. Luppo, R. Schaublin, M. Victoria, MRS Symp. Proc. 540 (1999) 539.
[19] F. Abe, M. Narui, H. Kayano, Mater. Trans., JIM 34 (11) (1993) 1053.
[20] H.L. Heinisch, M.L. Hamilton, W.F. Sommer, P.D. Ferguson, J. Nucl. Mater. 191–194 (1992) 1177.
[21] R.L. Fleischer, J. Appl. Phys. 33 (1962) 3504.
[22] Y. Dai, M. Victoria, MRS Symp. Proc. 439 (1996) 349.
[23] S.J. Zinkle, J. Nucl. Mater. 150 (1987) 140–158.
[24] H. Trinkaus, B. Singh, in press.
[25] W.L. Hu, D.S. Gelles, in: Proceedings of 13th Symposium on Influence of Radiation on Material Properties, ASTM STP 956, 1987, p. 83.
[26] R. Klueh, D.J. Alexander, J. Nucl. Mater. 187 (1992) 60.
[27] E.I. Materna-Morris, M. Rieth, K. Ehrlich, in: Proceedings of the 19th International Symposium on Effects of Irradiation on Materials, ASTM STP 1366, 2000, p. 597.